

On the origin of the Boson peak in globular proteins

Stefano Ciliberti*

CNRS; Univ. Paris Sud, UMR8626, LPTMS, ORSAY CEDEX, F-91405

Paolo De Los Rios, Francesco Piazza

LBS, Institute of Theoretical Physics - BSP-720, EPFL, CH-1015 Lausanne, Switzerland

(Received 00 Month 200x; in final form 00 Month 200x)

We study the Boson Peak phenomenology experimentally observed in globular proteins by means of elastic network models. These models are suitable for an analytic treatment in the framework of Euclidean Random Matrix theory, whose predictions can be numerically tested on real proteins structures. We find that the emergence of the Boson Peak is strictly related to an intrinsic mechanical instability of the protein, in close similarity to what is thought to happen in glasses. The biological implications of this conclusion are also discussed by focusing on a representative case study.

1 Introduction

The analogy between proteins and structural glasses has a long story and solid foundations. Among the different physical properties shared by the two classes of systems one can mention: (i) the anomalous specific heat [1]; (ii) the slow energy relaxation processes [2–4]; (iii) the existence of a dynamical transition as witnessed by the temperature dependence of the the atomic mean squared displacements [5, 6]; (iv) the excess of low frequency modes (the Boson Peak) in dynamical spectra obtained by inelastic neutron scattering experiments [7–9]. Although a somewhat generic explanation of the above experimental facts can be given in terms of a rugged energy landscape [10–12], a comprehensive explanation supported by solvable models is still missing. Incidentally, it is no surprise that proteins have been proposed as the paradigm of complexity in biological systems [13].

Here we focus on one of the glass-like features of proteins, the Boson Peak (BP). The latter is formally defined as the low frequency peak in the function $g(\omega)/g_D(\omega)$, where $g(\omega)$ is the vibrational density of states (DOS) as measured experimentally, and $g_D(\omega) \propto \omega^2$ is the Debye behavior in the $\omega \rightarrow 0$ limit. A peak in this function would then represent an excess of low vibrational modes with respect to a perfect harmonic crystal. The very origin of these new modes, related to the amorphous nature of the low energy configurations, has been the subject of a long debate in the recent years and yet there is no general agreement. As for structural glasses, people have proposed “soft-potential” theories including strong anharmonicities [14,15], harmonic lattices with random springs [16,17], extensions of standard mode coupling theory to the “frozen” state [18,19], and topologically disordered models [20,21]. Recently, the possibility that the BP is a universal feature of weakly connected systems has been suggested [22].

In this paper we will take the point of view that proteins can be considered to some extent as “random” structures, akin to those of structural glasses. In a sense, this constitutes our working hypothesis to be tested *a posteriori*. However, the rationale behind it can be identified in the empirical observation of the large scale structural properties of proteins. For instance, the pair correlation function of proteins at distances larger than $\approx 10 \div 15$ Å can be hardly distinguished from that of a set of points randomly distributed in an equivalent volume [23]. As a consequence, the “random” approximation is expected to work reasonably well for studying the behaviour of low frequency modes.

*Corresponding author. Email: Stefano.Ciliberti@roma1.infn.it. Now at Science & Finance, Capital Fund Management, 6 Blvd Haussmann, 75009 Paris, France.

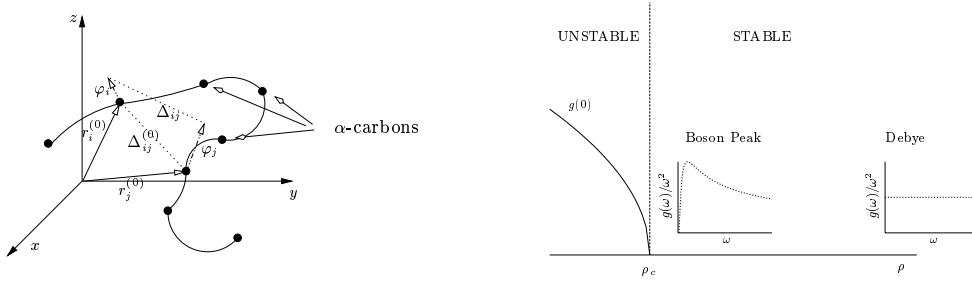


Figure 1. Left: Schematic cartoon of an Elastic Network Model. The protein is seen as a polymer-like chain coarse-grained at the amino-acid level with elastic pairwise interactions. Right: Pictorial representation of the phase diagram predicted by the ERM theory.

The rest of the paper is organized as follows. In section 2 we introduce the elastic network model of protein fluctuations and we briefly justify its usage in this context. In section 3 we discuss the harmonic approximation and the theoretical framework of the Euclidean Random Matrix (ERM) theory, whose main findings are also briefly summarized as a reference for the interpretation of our numerical results. In section 4 we report our results on the BP and on the role of the critical parameter, as well as a study of the relationship between functional modes and proteins' stability. Our comments and suggestions for further experimental studies are discussed in the last section.

2 Model building: Elastic Networks

The introduction of coarse-grained elastic network models in the context of protein dynamics is quite recent [24]. In fact, as a direct consequence of the known complexity of proteins' energy landscapes, all microscopic details are usually deemed essential to characterize their functional dynamics. As a result, people have long failed to realize that most features of the large- and medium-scale dynamics of proteins close to their native state, i.e. those related to biological function, can be successfully reproduced by simple harmonic interactions between amino-acids [25–28].

In our case, we aim at describing a universal feature of globular proteins at low frequency. Hence, the class of elastic network models appears *a fortiori* the correct choice to capture the main aspects of the BP phenomenology. In this spirit, the fine structural detail of microscopic interactions will be completely neglected, as well as the information contained in the amino-acid sequence. We thus coarse-grain the protein structure at the amino-acid level and replace each residue by a single particle whose equilibrium position coincides with that of the α -carbon as measured e.g. through X-ray crystallography. In practice, this amounts to dealing with a polymer folded exactly like the real protein. Each pair of particles falling within a fixed cutoff inter-distance are assumed to interact harmonically. More precisely, the global Hamiltonian of the system is (see the left panel of Fig. 1 for the notations):

$$\mathcal{H}[\{\mathbf{r}_i\}; \{\mathbf{r}_i^{(0)}\}] = \sum_{i,j} K(\Delta_{ij}^{(0)}) (|\Delta_{ij}| - |\Delta_{ij}^{(0)}|)^2. \quad (1)$$

The interaction stiffness can be also allowed to decrease smoothly with the pair distance as e.g. $K(\Delta_{ij}^{(0)}) = \kappa \exp[-(\Delta_{ij}^{(0)}/r_c)^2]$ (Gaussian model), but a sharp cutoff (i.e. stepwise) form of the type $K(\Delta_{ij}^{(0)}) = \kappa \Theta[r_c - \Delta_{ij}^{(0)}]$ could also be used. In this paper, we will adopt the Gaussian model.

The parameter κ sets the physical units for force constants, and is usually fixed by requiring the theoretical mean squared displacements of residues to match the experimental ones as determined from X-ray spectra for a given choice of the cutoff r_c [25, 26]. In principle, the latter should be tuned by fitting the low-frequency portion of experimental spectra at temperatures below the dynamical transition, where the protein fluctuates harmonically within the native minimum. However, such studies have never appeared in the literature to the best of our knowledge. The usual, cheaper alternative is to compare the theory with numerical spectra obtained by modeling the protein dynamics through all-atom force fields [27]. By doing so, one obtains $\rho_c \approx 3 \text{ \AA}$ in an all-atom representation, which reduces to $r_c \approx \langle N_a \rangle^{1/3} \rho_c \approx 8 \text{ \AA}$ when the protein structure is coarse-grained at the residue level. In the following, such value will be referred to as the optimal cutoff length scale.

3 Harmonic approximation and Euclidean Random Matrix Theory

Taking the harmonic approximation of the Hamiltonian (1) one is led to the quadratic form $\mathcal{H} \simeq \frac{1}{2}(\varphi, \mathcal{M}\varphi)$, where the Hessian matrix \mathcal{M} depends on the α -carbon coordinates $\{r_i^{(0)}\}$. As we anticipated in section 1, we will investigate the consequences of the hypothesis that these positions are random in space. Under this assumption, the matrix \mathcal{M} falls into the broad class of Euclidean Random Matrices [29]. In general terms, our problem amounts to taking N points at random in a volume V , assume that they interact according to some pair potential $v(r)$ and then compute the vibrational DOS of this *topologically disordered* system in the thermodynamic limit $N, V \rightarrow \infty$, while the density $N/V = \rho$ stays finite. After some efforts [20, 21, 30, 31], the following regimes have been identified under rather generic assumptions (see also the right panel of Fig. 1):

- $\rho \gg \rho_c$, high-density / low-temperature: the DOS is found to follow exactly the Debye behavior, $g(\omega) \propto \omega^2$. An amorphous solid behaves like a perfect crystal in the limit of very large density, meaning that an infinitely compact medium does not feel at all the presence of the disorder.
- $\rho \gtrsim \rho_c$: a peak in $g(\omega)/\omega^2$ emerges at ω_{BP} , where $\omega_{BP} \sim (\rho - \rho_c)$, and its height is found to diverge like $h_{BP} \sim (\rho - \rho_c)^{-1/2}$. This peak is identified with the BP and is due to the fact that the system “feels” the presence of a mechanical instability at ρ_c . The actual value of ρ_c depends on the details of the interaction.
- $\rho < \rho_c$: The characterization of the low density phase depends on the spatial nature of the interactions. In a vectorial model [21] the Hessian matrix has negative eigenvalues (i.e. imaginary frequencies). This phenomenon is usually referred to as a topological phase transition. The DOS at zero energy plays the role of an order parameter and one finds that $g(0) \sim (\rho_c - \rho)^{1/2}$.

To summarize, the system undergoes a phase transition, from a “solid” phase characterized by the minima of the energy surface, to a “liquid” phase where saddles become relevant for the high-frequency dynamics. If the Hessian matrix is positively defined and thus no negative modes are possible, the DOS in the liquid phase just reduces to a delta function at zero frequency [20]. It is also interesting to mention that the mean field exponents are consistent with the numerical findings on realistic glass-forming materials [31].

In view of applying this approach to our protein model, a control parameter has to be identified. The most natural choice is the interaction cutoff r_c . Given that the average connectivity $\langle c \rangle \sim \text{Tr} \mathcal{M} \sim r_c^3$, r_c is indeed a global measure of compactness of the protein. Very much like the temperature, this parameter is expected to signal the approach of an instability akin to a liquid-glass transition: if r_c is very large, the protein is extremely rigid and one expects its DOS to follow the Debye law. As r_c decreases, the protein looses stability and becomes an extremely flexible object, until it unfolds and eventually melts. If this idea is correct, one should detect a trace of this progressive structural change by looking at the vibrational DOS upon moving r_c . This is the problem we address in the next section.

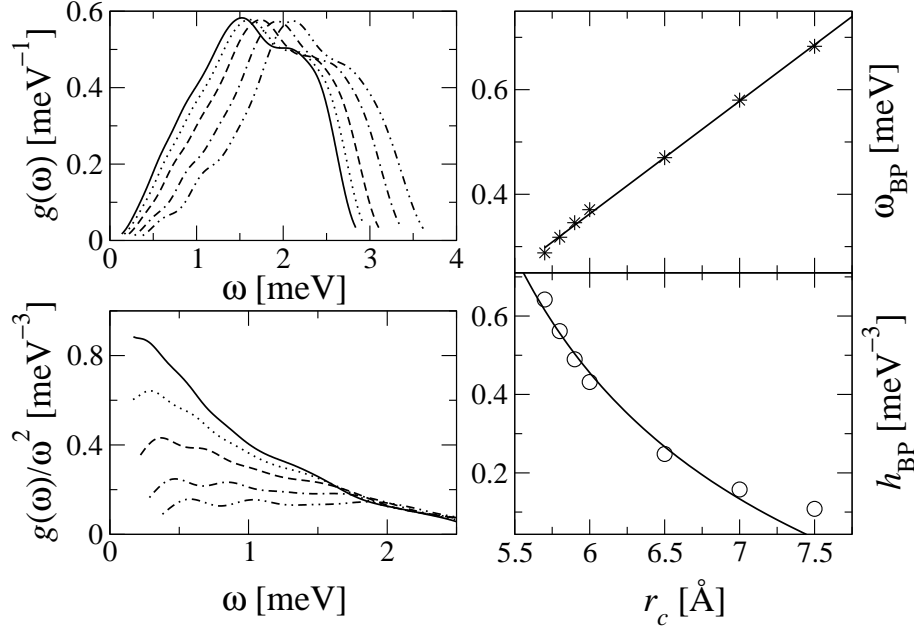


Figure 2. The BP phenomenology for the PDZ binding domain. Left panels: DOS and DOS divided by the Debye law. Solid line $r_c = 5.5$ Å, dotted line $r_c = 5.7$ Å, dashed line $r_c = 6$ Å, dot-dashed line $r_c = 6.5$ Å, dot-dot-dashed line $r_c = 7$ Å. Right panels: scaling of the BP frequency and height with the cutoff r_c . Solid lines represent the mean field prediction, $\omega_{BP} \sim (r_c - r_c^*)$, $h_{BP} \sim (r_c - r_c^*)^{-1/2}$.

4 Results

4.1 The Boson Peak

In Fig. 2 we report our results for the vibrational DOS of one particular protein out of the examined ensemble, namely the PDZ binding domain. In order to obtain a smooth and more reliable DOS, we generate a large number (order 10^3) of surrogates whose topology is compatible with the experimentally determined native structure [23]. The low frequency region shows a strong dependence on r_c , since a non-trivial excess of modes develops as a peak which eventually diverges for some critical r_c^* . We identify this peak as the BP. The position and height of the BP are plotted in the right panels versus the interaction cutoff r_c . The mean field predictions are also shown to perform reasonably well in the vicinity of the phase transition.

We have repeated this analysis on several proteins, choosing structures in a wide range of sizes (from 51 to 578 residues), and we always found an identical phenomenology. In order to clarify the physical origin of this behavior and its significance in biological terms, we investigate in the next subsection the role of the critical interaction cutoff r_c^* by measuring its correlation with structural properties of the protein.

4.2 The critical cutoff r_c^* : correlation with structural properties

In Table 1 we report measures of selected geometrical and structural indicators for a choice of proteins of different sizes, along with the correlations with the corresponding value of the critical cutoff distance r_c^* .

- We find a positive correlation between r_c^* and the number of residues N .
- We also find a positive correlation with a measure of the protein volume V estimated by constructing the equivalent ellipsoid according to the procedure described in ref. [32]. Such ellipsoid is characterized by three principal radii a_1 , a_2 and a_3 , which are obtained by diagonalising the symmetric matrix $\mathcal{A}_{\mu\nu} = \sum_i r_i^\mu r_i^\nu / N$, where $\mu, \nu = 1, 2, 3$ are Cartesian labels and r_i are the amino-acid coordinates. In the case of a continuous distribution of mass inside the ellipsoid, it can be shown that the three radii are simply given by $a_i = \sqrt{5\lambda_i}$, where $\lambda_1, \lambda_2, \lambda_3$ are the eigenvalues of the matrix \mathcal{A} .
- There clearly exists a negative correlation between r_c^* and the packing coefficient. The latter is a non-

dimensional measure of compactness defined as

$$p = \frac{4\pi}{3} \left(\frac{N}{V} \right) \left(\frac{d_0}{2} \right)^3$$

where $d_0 \simeq 3.83 \text{ \AA}$ is the distance between two consecutive residues along the protein main chain.

- The critical values r_c^* turn out to be positively correlated with the fraction of flexible residues. Such measure is calculated by flagging as highly fluctuating a residue whose average fluctuation over the first three slow modes is above its overall average fluctuation [33]. Average fluctuations over the first n modes are computed as

$$\langle |\vec{u}_i|^2 \rangle = \frac{3k_B T}{\kappa} \frac{1}{n} \sum_{k=1}^n \omega_k^{-2} \xi_i^k \xi_i^k$$

where ξ^k is the k -th eigenvector of the Hessian matrix and ω_k^2 the corresponding eigenvalue.

- Finally, a poor correlation is found between r_c^* and a combined measure of secondary structure content, defined as the fraction of residues classified either as from α -helices or β -sheets [34].

Overall, the measured correlations confirm that r_c^* is an *indirect measure of structural stability of a protein*, small values of r_c^* corresponding to highly compact (higher packing coefficient) and less flexible structures. Moreover, r_c^* is shown to increase with extensive quantities such as N and V , which may reflect the inherent increasing loss of globularity of larger structures. Surprisingly enough, the degree of secondary structure content does not prove to be an accurate indicator of stability in this sense. However, this only indicates that r_c^* is mostly sensitive to the large-scale degree of compactness, relevant to the robustness of the lowest vibrational modes. In other words, the local high stability of secondary motifs is not equivalent to the large-scale one as probed by r_c^* . This is also evident from the poor correlation (-0.19) existing between the secondary structure content and the packing coefficient p .

To be more clear, what we have found is that the excess of modes appearing in the low frequency region of a protein's DOS is a precursory feature that flags the approaching of a topological instability, whose meaning is to be traced back to the analogy with glass-forming materials. In particular, as it is the case for the Gaussian model in glasses [20, 21], such excess of modes should be interpreted as a precursor of the transition within a model that by definition becomes meaningless at the critical point. In fact, as the interaction cutoff r_c is decreased below the typical range of the first off-chain coordination shell, the model describes protein conformations that start loosening until they eventually unfold, thus becoming closer and closer to liquid-like assemblies of amino-acids. From a biological point of view, all that hints at an inherent effort of reconciling between spatial properties of liquids, i.e. increased degree of mobility, and the necessity of maintaining the structural stability of compact biological agents.

4.3 Critical cutoff and functional motions: the case of PDZ binding domains

The connection of the structural instability of a protein as revealed by the Boson peak analysis and the details of its functional dynamics is a matter of investigation deserving a systematic study on its own right. Here, we give an example of such analysis by sticking to the specific example of the PDZ binding domain.

Postsynaptic density-95/disks large/zonula occludens-1 (PDZ) interaction domains are crucial in regulating the cell dynamics. They play a fundamental role in signaling pathways by organizing networks of receptors and in targeting selected cellular proteins to multi-protein complexes [37–40]. Most PDZ-mediated interactions occur through the recognition of C-terminal peptide motifs by a large binding cleft built in the PDZ fold (see Fig. 3). Interestingly, experimental evidence from NMR measurements strongly suggests that the dynamics of PDZ domains upon ligand binding show correlations over the entire protein structure: this confirms the crucial role of collective low-frequency modes in the biological functions of proteins [41].

Table 1. Values of the critical cutoff distance r_c^* for different proteins and correlation with geometrical and structural indicators.

Protein	PDB-id	N	V (10^4 \AA^3)	p	% flex residues	$(\alpha + \beta)$ -fract.	r_c^* (\AA)
Insulin	4INS	51	0.75	0.20	27.45	0.53	4.57
Protein G	1PGB	56	0.76	0.21	37.50	0.70	3.64
Ubiquitin ^(a)	1UBI	71	1.04	0.20	35.21	0.46	3.53
PDZ binding domain ^(a)	1BFE	85	1.20	0.21	30.00	0.55	4.03
Lysozyme	166L	162	2.75	0.17	43.21	0.74	4.27
Adenylate Kinase	4AKE	214	5.41	0.12	50.93	0.64	7.85
LAO	2LAO	238	4.36	0.16	47.06	0.60	5.44
CYSB	1AL3	260	4.40	0.17	41.15	0.59	4.70
PBGD	1PDA	296	5.33	0.16	41.22	0.60	3.70
Thermolysin	5TLN	316	5.02	0.18	40.51	0.53	4.55
HSP70 ATP-binding domain	3HSC	382	7.49	0.15	38.74	0.66	5.28
Fab-fragment	1AE6	437	9.57	0.13	45.08	0.48	5.70
Serum Albumin	1A06	578	14.55	0.12	47.06	0.70	5.70
Correlation with r_c^*		0.45	0.52	-0.82	0.67	0.17	1

^a In these proteins short terminal tails of a few residues have been cut out in order to recover the correct low-frequency modes of the structure.

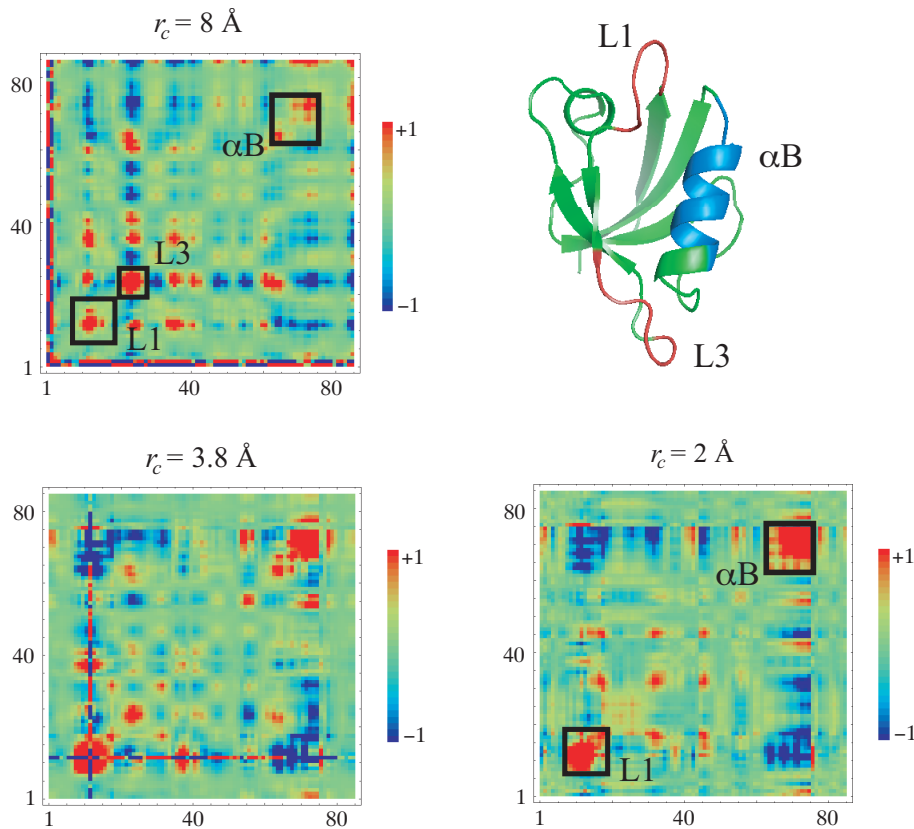


Figure 3. Pattern correlation plots of the second slowest normal mode as calculated through the Gaussian ANM model for the PDZ binding domain. The regions characterized by the largest displacements are highlighted and referenced explicitly within the protein structure. The functional motion corresponds to L1 and α B moving out of phase (cleft opening/closing).

In a previous work [36], a thorough normal-mode analysis of the PDZ binding dynamics has been performed by means of the CHARMM all-atom force field and of a recent version of the ANM, the $C\beta$ -ANM [42]. In such a model, also $C\beta$ carbons are considered and the complex chemical interactions between residues are described by springs connecting all $C\alpha$ - $C\alpha$, $C\alpha$ - $C\beta$, and $C\beta$ - $C\beta$ pairs whose distances in the native fold are smaller than $r_c = 7.5 \text{ \AA}$. The main result was that a single low-frequency mode captures the main spatial correlations characterizing the binding dynamics, namely a concerted opening of the hydrophobic pocket (see cartoon in Fig 3).

In order to investigate the correlation of such functional pattern with the general phenomenon of structural instability occurring as the density is lowered, we have looked for a mode with the same displacement

template within the Gaussian ANM model as a function of the parameter r_c . We observe that the known pattern is recovered in the second slowest mode, but only at relatively low values of r_c , whereas the mode loses cooperativity at larger values of the interaction cutoff. This is shown in Fig. 3, where we report correlation plots for $r_c = 2, 3.8$ and 8 Å. The correlation matrix C for mode k is defined as

$$C_{ij}^k = \sum_{\alpha=x,y,z} \xi_{i\alpha}^k \xi_{j\alpha}^k$$

where $\xi_{j\alpha}^k$ is the j -th component in direction α of the k -th normalized eigenvector, so that $-1 \leq C_{ij} \leq 1$.

Our results indicate that, as r_c is lowered towards the structural instability, the mode pattern becomes more and more pronounced. In particular, the loop L1 and the helix α B become rigid, anti-correlated units regulating the large-scale opening of the binding cleft. At the same time, the displacement of loop L3 correlated to L1 for tighter structures ($r_c = 8$ Å) gets strongly reduced. This result is a clear signature of the high robustness of large-scale functional motions. However, in order to assess the generality of our inferences, the same analysis should be repeated on a large pool of protein structures with known functional dynamics.

5 Conclusions and perspectives

In this paper we have addressed the Boson peak phenomenology experimentally observed in proteins by means of a simple elastic network model. After identifying the interaction cutoff as a control parameter, we have checked numerically the analytical predictions of ERM theory, already successfully reproduced by glass-forming materials. The BP turns out to be an intrinsic feature of proteins spectra as it is for structural glasses. On the same line, it signals the presence of a mechanical instability of the protein structure which can be related to the unfolding transition. However, in order to establish a precise relationship between BP divergence and unfolding transition, a more systematic study based on a sharp-cutoff elastic network model should be carried out.

To substantiate our interpretation of the BP emergence as related to the presence of an underlying mechanical instability, we have measured the correlation between the critical cutoff r_c^* and structural properties of the protein. The overall result indicates that r_c^* may serve as an indirect measure of global compactness of the protein, unrelated to the presence of local more stable motifs, such as secondary structures. Another fact to be stressed is that the critical r_c is always smaller than $7 \div 8$ Å, which is supposed to be the “correct” value for r_c obtained by comparing elastic network models with molecular dynamics spectra. Moreover, r_c^* is always greater than, or at worst of the order of, the distance between consecutive amino-acids along the backbone, ensuring that the loss of global stability does not interfere with the polymeric nature of proteins. As a rule of thumb, the larger r_c^* , the more unstable is the protein.

Taken together with the experimental fact that proteins are typically active in an environment whose local temperature is a few degrees smaller than the unfolding one, all these observations lead to a new interpretation of the surprising fact that proteins live more or less close to a phase transition. According to our analysis, in order to be efficient molecular machines able to perform their biological function, a protein has to keep a relative mechanical rigidity while being able to easily access the local minima directly connected to its native state. The BP is then the universal signature of such a trade-off. Interestingly, the observation that functional modes are those which “survive” in the critical regime strongly supports this interpretation.

We think that, in order to establish a deeper connection between the presence of the BP in proteins and this kind of theoretical approach, more experimental work is needed. The supposed relationship between the structural stability of a protein, its unfolding transition temperature, and its vibrational features certainly deserves a more detailed study. Furthermore, a systematic experimental approach to the BP phenomenology in proteins would allow to establish strength and limits of the ERM theory with respect to real systems. For the sake of concreteness, we would like to propose some ideas for experimental investigation of the BP phenomenon in proteins that may prove useful in probing the validity of our theoretical

framework.

In general, high pressure is a useful tool for the study of protein structure and dynamics [43]. More precisely, the effect of pressure on proteins is two-fold. Moderate pressures (< 0.4 GPa) cause elastic alterations in the spatial structure of the proteins, while further increase in pressure can cause the loss of the secondary structure along with the biological inactivation and denaturation. A number of pressure-dependent spectroscopic measurements have revealed non-trivial response of protein structures to pressure-induced stress, such as secondary structure-specific volume fluctuations and structure stabilization [44]. Moreover, normal mode calculations have also been successfully employed in such a context, showing that contributions to volume fluctuations from low frequency normal modes are typically found to dominate over those from higher frequency modes [45].

In view of the above facts, we propose to perform pressure-dependent measurements in the low-to moderate pressure regime to investigate the corresponding effect of density fluctuations on the BP frequency. In particular, combining vibrational spectroscopy with global experimental probes, such as adiabatic compressibility measurements and small angle X-ray scattering, should enable one to investigate experimentally the correlations between the critical interaction cutoff r_c^* and non-local structural indicators such as the packing coefficient.

Acknowledgments The work of S. C. is supported by EC through the network MTR 2002-00319, STIPCO.

References

- [1] J. L. Green, J. Fan, C. A. Angell, *J. Phys. Chem.* **98** 13780 (1994).
- [2] H. Frauenfelder, F. Parak, R. D. Young, *Ann. Rev. Biophys. Biophys. Chem.* **17** 451 (1988).
- [3] A. Xie, L. Van Der Meer, R. H. Austin, *J. Biol. Phys.* **28** 147 (2002).
- [4] F. Piazza, P. De Los Rios, Y.-H. Sanejouand, *Phys. Rev. Lett.* **94** 145502 (2005).
- [5] W. Doster, S. Cusack, W. Petry, *Nature* **337** 754 (1989).
- [6] I. E. T. Iben, *et al.*, *Phys. Rev. Lett.* **62** 1916 (1989).
- [7] A. Orecchini, A. Paciaroni, A. R. Bizzarri, S. Cannistraro, *J. Phys. Chem. B* **105** 12150 (2001).
- [8] H. Leyser, W. Doster, M. Diehl, *Phys. Rev. Lett.* **82** 2987 (1999).
- [9] W. Doster, S. Cusack, W. Petry, *Phys. Rev. Lett.* **65** 1080.
- [10] A. Ansari *et al.*, *Proc. Nat. Acad. Sci.* **82** 5000 (1985).
- [11] J. N. Onuchic, Z. Luthey-Schulten, P. G. Wolynes, *Ann. Rev. Phys. Chem.* **48** 545 (1997).
- [12] H. Frauenfelder, and D. T. Leeson, *Nature Struct. Biology* **5** 757 (1998).
- [13] H. Frauenfelder, *Proc. Nat. Acad. Sci.* **99** 2479 (2002).
- [14] U. Buchenau, Yu. M. Galperin, V. L. Gurevich, *Phys. Rev. B* **46** 2798 (1992).
- [15] V. G. Karpov *et al.*, *Sov. Phys. JETP* **57** 439 (1983).
- [16] W. Schirmacher, G. Diezemann, C. Ganter, *Phys. Rev. Lett.* **81** 136 (1998).
- [17] S. N. Taraskin, Y. L. Loh, G. Natarajan, S. R. Elliott, *Phys. Rev. Lett.* **86** 1255 (2001).
- [18] W. Götze, M. R. Mayr, *Phys. Rev. E* **61** 587 (2000).
- [19] T. Voigtmann, *J. Non-Cryst. Solids* **307** 188 (2002).
- [20] T. S. Grigera, V. Martín-Mayor, G. Parisi, P. Verrocchio, *Phys. Rev. Lett.* **87** 085502 (2001).
- [21] S. Ciliberti, T. S. Grigera, V. Martín-Mayor, G. Parisi, P. Verrocchio, *J. Chem. Phys.* **119** 8577 (2003).
- [22] M. Wyart, S. R. Nagel, T. A. Witten, *Europhys. Lett.* **72** 486 (2005).
- [23] S. Ciliberti, P. De Los Rios, F. Piazza, *Phys. Rev. Lett.* **96** (198103) (2006).
- [24] M. M. Tirion, *Phys. Rev. Lett.* **77** 1905 (1996).
- [25] A. R. Atilgan S. R. Durell, R. L. Jernigan, M. C. Demirel, O. Keskin, I. Bahar, *Biophys. J.* **80** 505 (2001).
- [26] T. Haliloglu *et al.*, *Phys. Rev. Lett.* **79** 3090 (1997).
- [27] K. Hinsen, *Proteins* **33** 417 (1998).
- [28] F. Tama and Y. H. Sanejouand, *Prot. Eng.* **14** 1 (2001).
- [29] M. Mézard, G. Parisi, A. Zee, *Nucl. Phys.* **B559** 689 (1999).
- [30] V. Martín-Mayor, M. Mézard, G. Parisi, P. Verrocchio, *J. Chem. Phys.* **114** 8068 (2001).
- [31] T. S. Grigera, V. Martín-Mayor, G. Parisi, P. Verrocchio, *Nature* **422** 289 (2003).
- [32] M. H. Hao, *et al.*, *Proc. Nat. Acad. Sci.* **89** 6614 (1992).
- [33] M. C. Demirel, O. Keskin, *J. Biomol. Struct. Dyn.* **22** 381 (2005).
- [34] D. Frishman, P. Argos, *Proteins* **23**(4) 566 (1995).
- [35] J. R. Banavar, A. Flammini, D. Marenduzzo, A. Maritan, A. Trovato, *Complexus* **1** 4 (2003).
- [36] P. De Los Rios, *et al.*, *Biophys. J.* **89** 14 (2005).
- [37] A. Y. Hung, M. Sheng, *J. Biol. Chem.* **277** 5699 (2002).
- [38] M. Sheng, C. Sala, *Annu. Rev. Neurosci.* **24** 1 (2001).
- [39] M. Zhang, W. Wang, **36530** (2003).
- [40] T. Pawson, P. Nash, *Science*. **300** 445 (2003).
- [41] E. J. Fuentes, C. J. Der, A. L. Lee, *J. Mol. Biol.* **335** 1105 (2004).
- [42] C. Micheletti, P. Carloni, A. Maritan, *Proteins* **55** 635 (2004).
- [43] K. Heremans, L. Smeller, *Biochim. Biophys. Acta*, **1386**, 353-370 (1998).
- [44] K. Akasaka, H. Li, H. Yamada, R. Li, T. Thoresen and CK Woodward, *Protein Science*, **8**(10) 1946-1953 (1999).
- [45] T. Yamato, J. Higo, Y. Seno and N. Go, *Proteins Struct. Funct. Genet.*, **16**, 327-340 (1993).